JOURNAL OF COMPUTATIONAL PHYSICS 33, 169–184 (1979)

Two-Layer Shallow-Water Flow in Two Dimensions, a Numerical Study

C. B. VREUGDENHIL

Delft Hydraulics Laboratory, Delft, The Netherlands

Received September 6, 1978; revised December 11, 1978

Two-layer shallow-water flow without mixing is discussed. The existence of two types of waves (surface and internal) with rather different velocities of propagation leads to a numerical approach with two separate grids. For that purpose, the differential equations are written in a weak-interaction form. Particular attention is paid to the formulation of boundary conditions leading to a mathematically well-posed and numerically stable problem. A slightly modified leap-frog method is shown to satisfy the requirements. Some examples are given, including salt-water intrusion in a schematic estuary.

1. PHYSICAL BACKGROUND

Several important problems in hydraulics are associated with nearly horizontal flows having a more or less pronounced two-layer structure. Some examples are: intrusion and circulation of salt sea water in estuaries, circulation of cooling water when discharged into rivers or lakes, and flow patterns in lakes or seas with stratification. In most cases there is no exact separation between the layers; rather, a schematization in terms of a two-layer system is made. From a physical point of view, it might be argued that a three-dimensional formulation is needed for such flows. However, an alternative two-dimensional method consuming less computer time is likely to remain attractive, even when time-dependent three-dimensional models come within the reach of computers. On the other hand, three-dimensional methods might meet with difficulties in resolving the steep gradients involved in a stratified flow structure.

Some work on two-dimensional two-layer systems has already been published [1, 3, 7, 13], generally based on methods for homogeneous (one-layer) flow. The only discussion of any extent concerning the particular features of two-layer systems is in [7].

The present work is of an exploratory nature. In particular, any effect of mixing between the layers is neglected, although it is relevant in most of the potential applications. Second, attention is confined to basins of a simple geometry, consisting of one or more rectangles. Extension to a more realistic geometry should preferably be based on a coordinate transformation, in order to retain the numerical advantages of straight boundaries. This paper is based on a more extensive report [12].

0021-9991/79/110169-16$02.00/0

2. Mathematical Formulation

The differential equations for two-layer flow in shallow water are obtained by vertically integrating the Reynolds equations for turbulent flow in three dimensions over each of the two layers, as shown in Fig. 1. The assumptions are the same as those normally made for the shallow-water equations. In particular, the Boussinesq approximation is made, stating that density variations are not important except in the pressure gradients.

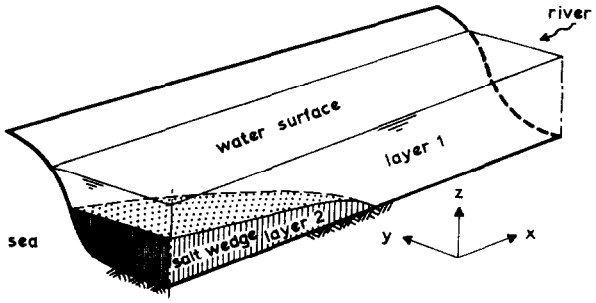

Fig. 1. Two-layer schematization.

The resulting equations are:

$$\frac{\partial a_1}{\partial t} + u_1 \frac{\partial a_1}{\partial x} + a_1 \frac{\partial u_1}{\partial x} + v_1 \frac{\partial a_1}{\partial y} + a_1 \frac{\partial v_1}{\partial y} = 0,$$

$$\frac{\partial a_2}{\partial t} + u_2 \frac{\partial a_2}{\partial x} + a_2 \frac{\partial u_2}{\partial x} + v_2 \frac{\partial a_2}{\partial y} + a_2 \frac{\partial v_2}{\partial y} = 0,$$

$$\frac{\partial u_1}{\partial t} + u_1 \frac{\partial u_1}{\partial x} + v_1 \frac{\partial u_1}{\partial y} + g \frac{\partial}{\partial x}(a_1 + a_2 + z_b) - f v_1 + \frac{\tau_{sx} - \tau_{ix}}{\rho_1 a_1} = 0,$$

$$\frac{\partial u_2}{\partial t} + u_2 \frac{\partial u_2}{\partial x} + v_2 \frac{\partial u_2}{\partial y} + g \frac{\partial}{\partial x}((1 - \epsilon) a_1 + a_2 + z_b) - f v_2 + \frac{\tau_{ix} - \tau_{bx}}{\rho_2 a_2} = 0,$$

$$\frac{\partial v_1}{\partial t} + u_1 \frac{\partial v_1}{\partial x} + v_1 \frac{\partial v_1}{\partial y} + g \frac{\partial}{\partial y}(a_1 + a_2 + z_b) + f u_1 + \frac{\tau_{sy} - \tau_{iy}}{\rho_1 a_1} = 0,$$

$$\frac{\partial v_2}{\partial t} + u_2 \frac{\partial v_2}{\partial x} + v_2 \frac{\partial v_2}{\partial y} + g \frac{\partial}{\partial y}((1 - \epsilon) a_1 + a_2 + z_b) + f u_2 + \frac{\tau_{iy} - \tau_{by}}{\rho_2 a_2} = 0$$

which can be combined in the quasi-linear form

$$\frac{\partial \mathbf{v}}{\partial t} + A \frac{\partial \mathbf{v}}{\partial x} + B \frac{\partial \mathbf{v}}{\partial y} + \mathbf{H} = 0, \tag{1}$$

where

$$\mathbf{v} = (a_1\,,\ a_2\,,\ u_1\,,\ u_2\,,\ v_1\,,\ v_2)^T,$$

$a_{1,2}$ is the thickness of upper and lower layer, $u_{1,2}$ and $v_{1,2}$ are velocity components in each layer, x and y are horizontal coordinates, t is time, g is acceleration due to gravity, ϵ is the relative density difference $(\rho_2 - \rho_1)/\rho_1$, f is the Coriolis parameter, z_b is the bottom level, τ_s is the surface (wind) stress, τ_i is the interfacial shear stress $-\rho k_i(u^2 + v^2)^{1/2}(u, v)$, and τ_b is the bottom shear stress $\rho k_b(u_2^2 + v_2^2)^{1/2}(u_2\,,\ v_2)$.

The system (1) is hyperbolic under the condition

$$u^2 + v^2 \leqslant \epsilon g h, \tag{2}$$

where $(u, v) = (u_2 - u_1\,,\ v_2 - v_1)$ is the relative velocity and $h = a_1 + a_2$ is the total depth.

This condition can be interpreted as a physical stability condition: if it is violated, the equations have exponentially growing solutions. The matrices A and B are not symmetric and, more importantly, cannot simultaneously be brought into a symmetric form by a similarity transformation.

The physical behavior of the system (1) is brought out by considering wavelike solutions of the equations with constant coefficients A and B, and $\mathbf{H} = 0$:

$$v \sim \exp\{i(k_x x + k_y y - \omega t)\}. \tag{3}$$

The velocities of propagation $c = \omega k^{-1}$ with $k^2 = k_x^2 + k_y^2$ are the eigenvalues of the matrix $k^{-1}(k_x A + k_y B)$. A very good approximation for small values of ϵ is:

convective type:

$$\begin{aligned} c_1 &= \mu_1\,, \\ c_2 &= \mu_2\,; \end{aligned} \tag{4}$$

internal waves:

$$c_{3,4} = a\mu_2 + (1 - a)\,\mu_1 \pm \{a(1 - a)(\epsilon g h - (\mu_1 - \mu_2)^2)\}^{1/2}; \tag{5}$$

surface waves:

$$c_{5,6} = a\mu_1 + (1 - a)\,\mu_2 \pm (gh)^{1/2}, \tag{6}$$

where

$$\begin{aligned} a &= a_1/h, \\ \mu_{1,2} &= k^{-1}(k_x u_{1,2} + k_y v_{1,2}). \end{aligned} \tag{7}$$

The stability condition (2) ensures that the internal-wave speeds $c_{3,4}$ are real for all wavenumbers. The internal-wave speeds are a factor of 10 to 30 smaller than the

surface-wave speeds $c_{5,6}$, assuming representative values of ϵ from 0.001 to 0.04. This difference in propagation speed is an invitation to use different numerical methods for surface and internal waves (Section 4). For that purpose, it is attractive to split the system of differential equations into two separate systems. In a linear version of the equations, this has been done by Veronis [11]. The present nonlinear system does not appear to allow a complete separation, but a "weak interaction" form can be obtained by introducing the following dependent variables:

external variables:

$$\begin{aligned} h &= a_1 + a_2 , \\ p &= a_1 u_1 + a_2 u_2 , \\ q &= a_1 v_1 + a_2 v_2 ; \end{aligned}$$

internal variables:

$$\begin{aligned} a &= a_1 h^{-1}, \\ u &= u_2 - u_1 , \\ v &= v_2 - v_1 . \end{aligned}$$

These differ from the variables used by Veronis only by $O(\epsilon)$. The following weakly coupled systems result:

surface waves

$$\frac{\partial h}{\partial t} + \frac{\partial p}{\partial x} + \frac{\partial q}{\partial y} = 0, \tag{8a}$$

$$\frac{\partial p}{\partial t} + \frac{\partial}{\partial x}\left(\frac{p^2}{h} + \frac{1}{2} g h^2\right) + \frac{\partial}{\partial y}\left(\frac{pq}{h}\right) - fq + gh \frac{\partial z_b}{\partial x} - \frac{\tau_{sx}}{\rho_1} + \frac{\tau_{bx}}{\rho_2}$$

$$= - \frac{\partial}{\partial x}\{ha(1 - a) u^2\} - \frac{\partial}{\partial y}\{ha(1 - a) uv\} + \epsilon g(1 - a) h \frac{\partial}{\partial x}(ah), \tag{8b}$$

$$\frac{\partial q}{\partial t} + \frac{\partial}{\partial x}\left(\frac{pq}{h}\right) + \frac{\partial}{\partial y}\left(\frac{q^2}{h} + \frac{1}{2} g h^2\right) + fp + gh \frac{\partial z_b}{\partial y} - \frac{\tau_{sy}}{\rho_1} + \frac{\tau_{by}}{\rho_2}$$

$$= - \frac{\partial}{\partial x}\{ha(1 - a) uv\} - \frac{\partial}{\partial y}\{ha(1 - a) v^2\} + \epsilon g(1 - a) h \frac{\partial}{\partial y}(ah); \tag{8c}$$

internal waves

$$\frac{\partial a}{\partial t} + \frac{\partial}{\partial x}\left\{\frac{pa}{h} - a(1 - a)u\right\} + \frac{\partial}{\partial y}\left\{\frac{qa}{h} - a(1 - a)v\right\}$$

$$= a\left\{\frac{\partial}{\partial x}\left(\frac{p}{h}\right) + \frac{\partial}{\partial y}\left(\frac{q}{h}\right)\right\} + \frac{a(1 - a)}{h}\left\{u \frac{\partial h}{\partial x} + v \frac{\partial h}{\partial y}\right\}, \tag{9a}$$

$$\frac{\partial u}{\partial t} + \frac{\partial}{\partial x}\left\{\frac{pu}{h} + \left(a - \frac{1}{2}\right)u^2 - \epsilon gah\right\} + \left\{\frac{q}{h} - (1-a)v\right\}\frac{\partial u}{\partial y} + v\frac{\partial}{\partial y}\left(\frac{p}{h} + au\right)$$

$$- fv + \frac{\tau_{sx}}{\rho_1 ah} + \frac{\tau_{bx}}{\rho_2(1-a)h} - \frac{\tau_{ix}}{\rho ha(1-a)} = 0, \tag{9b}$$

$$\frac{\partial v}{\partial t} + u\frac{\partial}{\partial x}\left(\frac{q}{h} + av\right) + \left\{\frac{p}{h} - (1-a)u\right\}\frac{\partial v}{\partial x} + \frac{\partial}{\partial y}\left\{\frac{qv}{h} + \left(a - \frac{1}{2}\right)v^2 - \epsilon gah\right\}$$

$$+ fu + \frac{\tau_{sy}}{\rho_1 ah} + \frac{\tau_{by}}{\rho_2(1-a)h} - \frac{\tau_{iy}}{\rho ha(1-a)} = 0. \tag{9c}$$

By differentiation, these equations can be brought in the quasi-linear form, to be used for theoretical analysis:

$$\frac{\partial \mathbf{v}_s}{\partial t} + A_s\frac{\partial \mathbf{v}_s}{\partial x} + B_s\frac{\partial \mathbf{v}_s}{\partial y} + \mathbf{H}_s = \boldsymbol{\delta}_s(\mathbf{v}_s, \mathbf{v}_i), \tag{8d}$$

$$\frac{\partial \mathbf{v}_i}{\partial t} + A_i\frac{\partial \mathbf{v}_i}{\partial x} + B_i\frac{\partial \mathbf{v}_i}{\partial y} + \mathbf{H}_i = \boldsymbol{\delta}_i(\mathbf{v}_s, \mathbf{v}_i), \tag{9d}$$

where $\mathbf{v}_s = (h, p, q)^T$ and $\mathbf{v}_i = (a, u, v)^T$.

The right-hand members $\boldsymbol{\delta}_{s,i}$ of (8) and (9) are small in a certain sense, although it is not easy to show this in a mathematically formal way. Two special cases are worth mentioning:

1. If $\epsilon = 0$ and $u = v = 0$, the system (9) degenerates and (8) becomes identical with the usual shallow-water equations.

2. If $z_b + h$ = constant and $p = q = 0$, the "rigid-lid" approximation is obtained in which only (9) remains. This is effectively what has been done in, e.g., [4]. The resulting system is very similar to the shallow water equations, particularly if a_2/h is small.

It is noted that Eqs. (8a)–(8c) are in a conservative form except for the interaction terms $\boldsymbol{\delta}_s$. System (9) apparently cannot be written in such a form, unless the flow is exactly in one dimension (i.e., parallel to the x-axis). This is important for the representation of discontinuous (shocklike) solutions (Section 5). Finally, it is noted that, unlike the complete system (1), A_s and B_s can be symmetrized simultaneously. The same applies to A_i and B_i.

3. Boundary Conditions

In most applications, curved boundaries occur. These may be closed boundaries in the form of coastlines, or open boundaries which terminate the model at a more or less arbitrary location. In the latter case, any effect of the "outside world" has

to be represented in the boundary conditions. Here, only straight boundaries are discussed, with the idea of transforming any curved boundaries into straight ones by a suitable coordinate transformation. There are some indications that this might be a more satisfactory procedure than the common approximation of a curved boundary by straight-line segments through the nearest grid points. Moreover, a theoretical analysis of the boundary-value problem is practicable only for straight boundaries. As indicated in [5], the analysis can be done for the restricted problem of linear equations for a semi-infinite region. Conditions for well-posedness can then be transferred to the original boundary-value problem.

Without loss of generality, let us assume that a boundary is located at $x = 0$. The number of boundary conditions, necessary to determine the solution then equals the number of "in-going" characteristics [2, 5] obtained from (4), (5), and (6) with $k_y = 0$. This leads to the conclusion that none to six boundary conditions are needed, depending on the signs of the characteristic speeds.

Apart from these necessary conditions, an energy argument can give sufficient conditions to have a well-posed problem (e.g., [10]). As already mentioned, system (1) cannot be symmetrized, but the separate systems (8) and (9) can be written in a symmetric form, at least in the constant-coefficient case which is the case considered here. For example,

$$\begin{aligned} \mathbf{v}' &= T\mathbf{v}_i, \\ A' &= TA_iT^{-1}, \\ B' &= TB_iT^{-1} \end{aligned}$$

with symmetric A' and B'. For the internal waves,

$$T = \begin{pmatrix} m\{a(1-a)\}^{-\frac{1}{2}} & 0 & 0 \\ 0 & n & uvn^{-1} \\ 0 & 0 & mn^{-1} \end{pmatrix}$$

with $m = \{\epsilon gh(\epsilon gh - u^2 - v^2)\}^{1/2}$ and $n = (\epsilon gh - v^2)^{1/2}$.

Equation (9) becomes (disregarding $\mathbf{H}_i$)

$$\frac{\partial \mathbf{v}'}{\partial t} + A'\frac{\partial \mathbf{v}'}{\partial x} + B'\frac{\partial \mathbf{v}'}{\partial y} = 0. \tag{10}$$

Defining an internal product of two vector functions u and v on the region S as

$$(u, v) = \iint_S u^T v \, dx \, dy$$

and a norm $\| \mathbf{v} \|^2 = (v, v)$, Eq. (10) yields, after premultiplication by $\mathbf{v}'^T$,

$$\frac{\partial}{\partial t}\| \mathbf{v}' \|^2 + [\mathbf{v}'^T A' \mathbf{v}']_{x=0}^{X} + [\mathbf{v}'^T B' \mathbf{v}']_{y=0}^{Y} = 0.$$

A sufficient condition for well-posedness is that each contribution from the boundaries is negative. For example, on the boundary $x = 0$ we should have

$$F \equiv [\mathbf{v}'^T A' \mathbf{v}']_{x=0} < 0 \tag{11}$$

for homogeneous boundary conditions. A' can be diagonalized by another transformation $A' = R^T D R$ and characteristic variables w are defined by $\mathbf{w} = R\mathbf{v}' = RT\mathbf{v}_i$ and we find

$$F = c_1^* w_1^2 + c_3 w_2^2 + c_4 w_3^2. \tag{12}$$

Note that the first eigenvalue, which proves to be $c_1^* = (2a - 1)\, u$, does not conform to c_1 or c_2, which is a consequence of neglecting the interaction terms. The following cases can be discerned to satisfy Eq. (11), depending on the parameter

$$\phi = (2a - 1)u\{a(1 - a)(\epsilon g h - u^2)\}^{-1/2}$$

which is the ratio between the term common to c_3 and c_4 (Eq. (5)) and the term occurring with opposite signs:

1. Supercritical outflow $\phi \leqslant -1$

$$c_4 \leqslant c_1^* \leqslant c_3 \leqslant 0,$$

no boundary conditions.

2. Subcritical outflow $-1 < \phi \leqslant 0$

$$c_4 \leqslant c_1^* \leqslant 0 < c_3 .$$

One boundary condition of the form

$$w_2 = \alpha w_3 + \beta w_1$$

can be imposed under the restriction

$$\phi\alpha^2 + (\phi - 1)\,\beta^2 \geqslant -\phi(\phi - 1)(\phi + 1)^{-1}. \tag{13}$$

In particular $\alpha = \beta = 0$ is allowed.

3. Subcritical inflow $0 < \phi \leqslant 1$

$$c_4 \leqslant 0 < c_1^* \leqslant c_3 .$$

Two boundary conditions of the form

$$w_2 = \alpha w_3 , \qquad w_1 = \beta w_3$$

can be imposed under the restriction

$$(\phi + 1)\,\alpha^2 + \phi\beta^2 \leqslant 1 - \phi. \tag{14}$$

4. Supercritical outflow $\phi > 1$

$$0 < c_4 \leqslant c_1^* \leqslant c_3\,.$$

All three characteristic variables w_i are prescribed, which gives $F = 0$ for homogeneous boundary conditions.

This set of boundary conditions is completely analogous to and can be used together with that for surface waves [10] resulting from Eq. (8). The characteristics c_1^* of (9) and the corresponding c_2^* of (8) differ from the correct values c_1 and c_2 (Eq. (4)), Hence, by analogy, the boundary conditions associated with those two characteristics can be formulated as

if $c_1 > 0$ and $c_2 > 0$:	prescribe q and v;
if $c_1 c_2 \leqslant 0$ and $p > 0$:	prescribe q;
$p \leqslant 0$:	prescribe v;
if $c_1 \leqslant 0$ and $c_2 \leqslant 0$:	no boundary condition.

Due to neglecting the interaction terms, there is no guarantee that this set of boundary conditions is sufficient for well-posedness of system (1). However, we believe that it is the most sensible choice which can be made with the available information.

The boundary conditions formulated in terms of characteristic variables w_i have a clear physical meaning, at least for the components associated with $c_3, \ldots, c_6$. They can be identified with incident and reflected waves. The general rule is that incident waves are specified, either directly as a function of time ($\alpha = \beta = 0$) or in terms of outgoing waves.

Finally, it must be stressed that the above analysis applies to the linearized equations only. It can be expected to be valid for the nonlinear case also, provided that the solution remains sufficiently smooth. However, there are at least two effects which may destroy smoothness: (1) discontinuous solutions can occur, and (2) short waves may be generated by nonlinear effects in a way similar to the energy cascade in turbulence. Nonlinear stability, therefore, remains an open question.

4. Numerical Method

The choice of a numerical method is based on the effort required to obtain the solution with a certain accuracy, within the bounds of stability considerations. The effort includes not only computer requirements but also programming and therefore

is somewhat subjective. For a wave-propagation problem, accuracy can be formulated very well in terms of amplitude and phase errors, obtained from a linear analysis (see, e.g., [5]). If the (linearized) differential equations have solutions of the form

$$\mathbf{v} = \mathbf{v}_0 \exp\{ik(x - ct)\},$$

the solutions of the finite-difference equations can be written as

$$\mathbf{v} = \mathbf{v}_0 \exp\{ik(x - c_r ct) - kct(2\pi)^{-1} \ln d\},$$

where $d = |\rho|^{2\pi/(\sigma\xi)}$ is the wave damping factor per wave period, $c_r = -\arg(\rho)(\sigma\xi)^{-1}$ is the relative velocity of propagation, $\xi = k\Delta x = 2\pi/N$, Δx is the mesh width, Δt is the time step, $\sigma = c\Delta t/\Delta x$ is the Courant number, and ρ is the amplification factor.

For simplicity, a one-dimensional case is considered, but the results are assumed

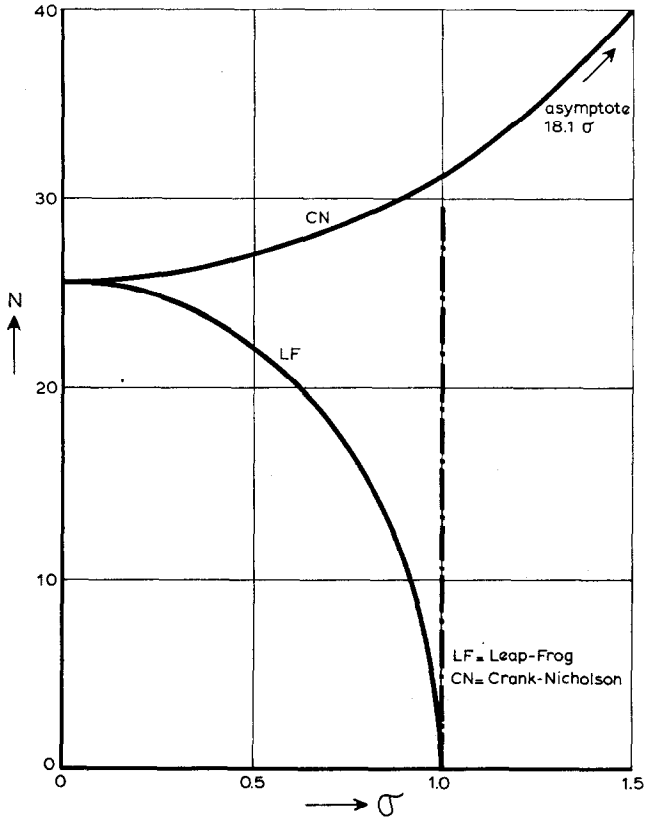

FIG. 2. Number of points per wavelength N for 1 % accuracy with leap-frog and Crank–Nicholson methods.

to be valid in two dimensions at least in order of magnitude. For each finite-difference method, values of d and c_r can be found as functions of σ, N, and any other free parameters. If a certain accuracy limit ϵ is set, so that $| 1 - d | < \epsilon$ and $| 1 - c_r | < \epsilon$, the required number N of points per wavelength can be plotted as a function of the Courant number σ (Fig. 2).

Two typical second-order accurate methods are illustrated: the Crank–Nicholson method (CN) and the leap-frog method (LF). An advantage of the former is the possibility to use a Courant number exceeding unity. The price to be paid is an increase in the number of grid points per wavelength. Actually, if the effort is defined as the total number of computer operations, it is easy to show that it is inefficient to use a Courant number much higher than unity. Nevertheless, in the present case it is possible to solve the surface-wave equations by CN and the internal-wave equations by LF (analogous to [7]) so that both operate with the same time step Δt. Another, more efficient, method is to use LF for both wave types but on different grids, as shown in Fig. 3. If the ratio of $\Delta t/\Delta x$ for the two wave types is chosen to be of the

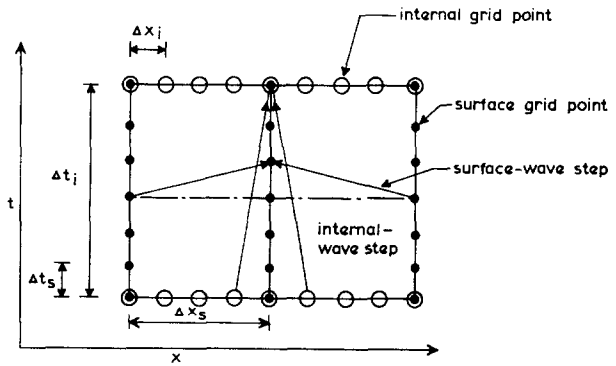

FIG. 3. Grids and interpolation (for simplicity y-direction is not shown).

order of the ratio of the wave speeds, both work at approximately equal values of the Courant number, which is then limited only by stability considerations. This is an effective method, unless the mesh width is dictated by other considerations, such as representation of geometrical details.

The procedure is to apply the leap-frog method to Eqs. (8) and (9) on two separate grids, interpolating the interaction terms at those grid points where they are not defined (Fig. 3). A linear interpolation procedure is chosen, which formally destroys second-order accuracy, but for practical values of the mesh width the first-order interpolation error is not important compared to the second-order discretization error.

It is relatively simple to show that the leap-frog method is stable with closed boundaries, under the usual condition

$$2 \mid c_{\max} \mid \Delta t/\Delta x \leqslant 1 \qquad (\Delta x = \Delta y) \tag{15}$$

which is $2^{1/2}$ times more restrictive than the condition resulting from a Von Neumann

stability analysis for the pure initial-value problem. With open boundaries, the leap-frog method may be unstable [8]. To overcome this difficulty, the following modification is used [6, 9]:

$$D_{0t}v + A(Q_{1x}\bar{\mathbf{v}} + Q_{2x}\mathbf{v}) + B(Q_{1y}\bar{\mathbf{v}} + Q_{2y}\mathbf{v}) + \bar{\mathbf{H}} = 0, \tag{16}$$

where

$$\begin{aligned} D_{0t}\mathbf{v} &= \{\mathbf{v}(x, t + \Delta t) - \mathbf{v}(x, t - \Delta t)\}(2\Delta t)^{-1}, \\ \bar{\mathbf{v}} &= \tfrac{1}{2}\{\mathbf{v}(x, t + \Delta t) + \mathbf{v}(x, t - \Delta t)\}, \\ Q_x\mathbf{v} &= \{\mathbf{v}(x + \Delta x, t) - \mathbf{v}(x - \Delta x, t)\}(2\Delta x)^{-1} \qquad (x \geqslant \Delta x) \\ &= \{\mathbf{v}(x + \Delta x, t) - \mathbf{v}(x, t)\}\,\Delta x^{-1} \qquad (x = 0), \end{aligned} \tag{17}$$

and Q_{1x} is the symmetric part of the operator Q_x (similar for Q_y). It can be shown by a standard argument [8] that this method is stable for linear equations under condition (15) and assuming the continuous problem to be wellposed, which is the case if the boundary conditions are treated as discussed in the preceding section. The operator Q_{1x} involves only points on the boundary $x = 0$ and at $x = \Delta x$, so that implicit equations result from Eq. (16) at the boundaries only, involving not more than two grid points at a time. These implicit equations are nonlinear, but they can be linearized in each time step without affecting the accuracy.

A less desirable property of the leap-frog method is the occurrence of undamped parasitic solutions with a period $2\Delta t$, which may give rise to a "time splitting" phenomenon. In one-dimensional problems, this is associated with short waves (wavelength $2\Delta x$). In two dimensions, short period waves are also possible with a larger wavelength. A wave with an amplification factor $\rho = -1$ can occur if

$$\det(iA \sin \xi + iB \sin \eta) = 0$$

and for relatively long waves ($\xi = k_x \Delta x$ and $\eta = k_y \Delta y$ small) this happens if

$$k_x u_{1,2} + k_y v_{1,2} = 0,$$

i.e., for waves propagating at right angles to the flow vector. A spatial dissipation process scarcely affects such waves, so that the only way to suppress them appears to be a time-averaging process every nth time step. This turns out to be necessary in some of the applications. It must be borne in mind that this averaging process, together with the associated restart procedure, does affect accuracy of the method, but this is not elaborated here.

The interface may intersect the bottom ($a = 1$) or the free surface ($a = 0$), thus separating two-layer regions from one-layer regions. Unlike some meteorological applications (such as [4]) where the surface front is quite important, in most hydraulic applications it is sufficient to have the approximate position of such fronts.

For that purpose, it is noted that Eqs. (8) and (9) are valid formally if $a = 0$ or 1, together with $u = v = 0$, provided the bottom and interface stresses vanish. Therefore, a very simple method has been used by setting a to one of its extreme values 0 or 1 whenever it exceeds these, and setting $u = v = 0$ at the same time. In a very thin layer near these limits, the stresses are multiplied by a function of the layer thickness a which forces them to zero if $a = 0$ or 1. In the examples shown in this paper, this method works well in the sense that errors in the overall mass balance do not exceed 1 or 2%. However, on a closer examination of the procedure, it is seen that the local continuity errors are systematic and indeed long-term computations with a one-dimensional variant of the model have shown that the overall mass balance can be violated quite seriously. For the leap-frog method, or any other explicit method, no method of treating the surface fronts in a mass-conserving way, simpler than using frontmarkers as in [4] has yet been found.

5. Application

The examples discussed here do not serve to prove the correctness of the results, but rather to indicate the possibilities. In addition, some mathematical checks have been made for situations in which an (approximate) analytical solution is available, such as linear wave propagation and one-dimensional steady flow under wind influ-

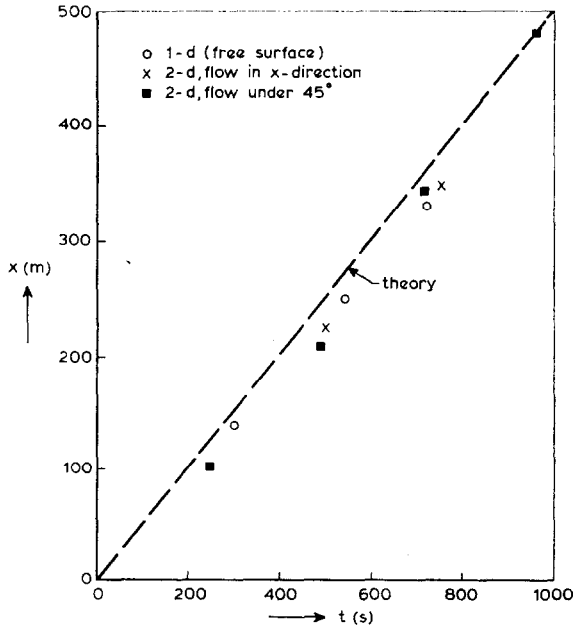

FIG. 4. Path of a discontinuity in the interface, according to theory and to 1-d and 2-d computations.

ence [12]. In all the examples shown, boundaries parallel to the x-axis are vertical walls, on which the normal component of velocity is zero.

An example of some theoretical interest is the propagation of internal discontinuities. The one-dimensional form of Eq. (9) allows weak solutions with discontinuities, the propagation speed of which can be derived from integral relations. For an internal front advancing over a stationary layer ($a = a_0$, $u = v = 0$ ahead of the front, $a = a_+$ behind) the result is

$$c = a_+(1 - a_+)(\epsilon g h)^{1/2}\{a_+(1 - a_+) + (a_+ - \tfrac{1}{2})(a_+ - a_0)\}^{-1/2} \tag{18}$$

in reasonable agreement with measurements. In Fig. 4 some numerical experiments are compared with the theoretical value of Eq. (18). They include one-dimensional computations and two-dimensional cases in which the flow is either in the x-direction or at 45° to it. In the latter case, the nonconservative form of the equations (cf. Section 2) shows up and some difficulties might be expected.

As seen from Fig. 4, however, there is no sign of disagreement with the theory, at least for the rather crude schematization used here. A fourth-order dissipation process in both x- and y-directions has been applied after each time step. No time averaging has been necessary.

As an example of a practically important case, consider an estuary as shown in Fig. 5. At $x = 0$, the area is connected to the open sea, from which a running tidal

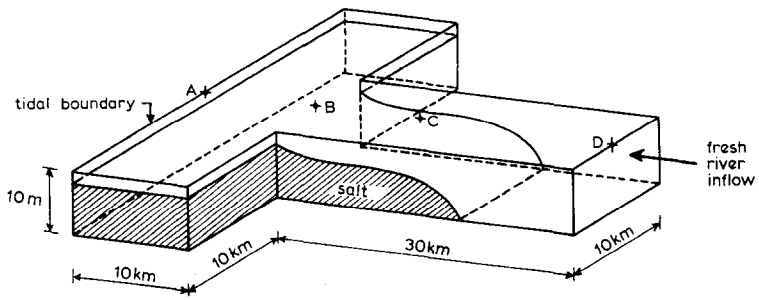

FIG. 5. Schematic estuary.

wave is assumed to come in, propagating in the x-direction. At $x = 40$ km, a river flows into the basin. Its discharge and water depth far upstream are assumed to be constant. The salt wedge is assumed not to reach the upstream boundary. Boundary conditions, applied at $x = 0$ are,

$$p - p_0 - p_1\phi(t) + \{-P/H + (gH)^{1/2}\}\{h - h_0 - h_1\phi(t)\} = 0, \tag{19}$$

$$\{A(1 - A)\}^{1/2}(\epsilon gH - U^2)^{-1/2}(u - u_0) - (a - a_0) = 0 \tag{20}$$

with

$$\phi(t) = \{1 - \exp(-(t/T_1)^2)\} \sin(2\pi t/T).$$

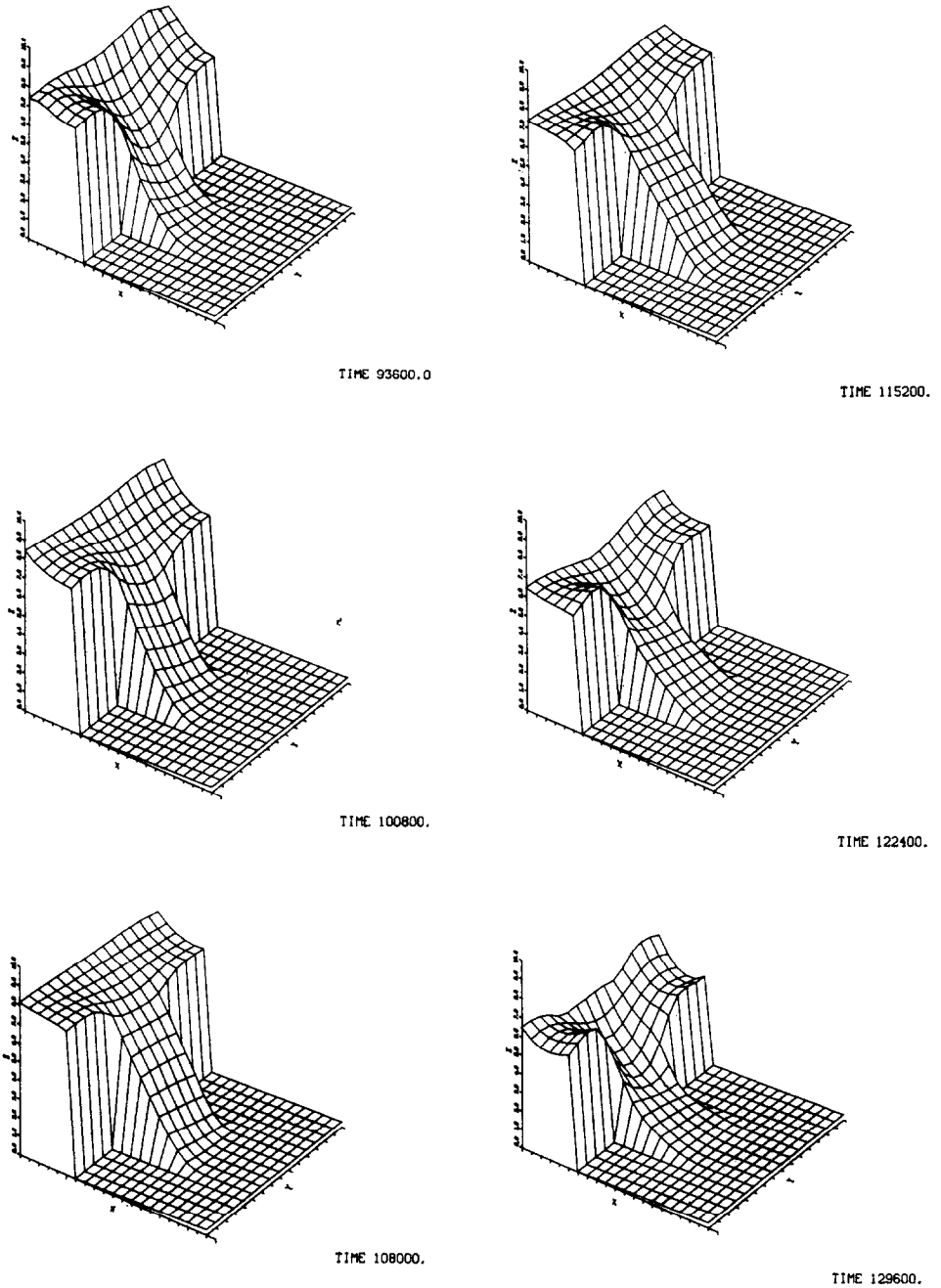

FIG. 6. Interface position in estuary of Fig. 5 at 2-h intervals during the third tidal cycle.

Quantities in Eqs. (19) and (20) indicated by capitals are evaluated at the central time level of the leap-frog scheme so that linear boundary conditions result. At the upstream boundary the condition corresponding to (19) is

$$p - p_r - \{P/H + (gH)^{1/2}\}(h - h_r) = 0, \tag{21}$$

where p_r and h_r are discharge and depth far upstream. Where necessary, at in-flow $q = 0$ or $v = 0$ is applied according to Section 3. Some numerical data are:

$h_0 = 10$ m
$h_1 = 0.75$ m
$p_0 = -1.667$ m^{2}s^{-1}
$p_1 = h_1(gh_0)^{1/2}$
$h_r = 10$ m
$p_r = -5$ m^{2}s^{-1}
$u_0 = 0.5555$
$a_0 = 0.3$

$T = 0.45 \times 10^5$ s
$T_1 = 2 \times 10^4$ s
$f = 10^{-4}$ s^{-1}
$\epsilon = 0.04$
$k_i = 0.4 \times 10^{-3}$
$k_b = 0.4 \times 10^{-2}$
$\tau_s = 0$

$\Delta t = 90$ s
$\Delta x = 2000$ m
$\Delta y = 2000$ m.

A common grid is used for surface and internal waves in order to have a reasonable resolution for both. Time-averaging is applied every hour (40 time steps); otherwise quite large oscillations are obtained, particularly in the internal variables. As an initial condition, an estimated equilibrium flow without tide is used. After a few tidal cycles, an approximately periodic flow is produced which is practically independent of the initial condition. Figure 6 shows some pictures of the interface position during the third tidal cycle. Quantitative conclusions cannot be drawn from the results but they are reasonable in a qualitative sense.

The example of Figs. 5 and 6, comprising about 160 grid points and 1500 time steps took about 1000 s CPU time on a CDC 6600, corresponding to about 1500 (variables) $\times$ (grid points) $\times$ (time steps)/s CPU time. No attempt was made to optimize the program.

6. Conclusion

A formulation and analysis have been given for two-layer shallow-water flow without mixing. Although the behavior of such a system is analogous to homogeneous shallow-water flow, some differences have been put forward which influence the choice of a numerical method. The velocities of propagation of surface and internal waves differ by an order of magnitude which leads to the application of two separate grids. A weak-interaction form of the equations makes this possible. Particular attention has been given to the boundary conditions, concerning both the number and the type of conditions leading to a well-posed problem, and to numerical stability. Because of the asymmetry of the equations, a rigorous analysis has not been possible, but

useful indications are obtained from the two subsystems with interaction terms neglected. The results are confirmed by some numerical tests which yield qualitatively, and in some simple cases also quantitatively, useful results.

A comprehensive verification of the mathematical formulation has not yet been done. Important difficulties are not to be expected in the two-layer model as such, but rather in the semiempirical terms representing surface, bottom, and interfacial shear stress. Moreover, in most practical applications, mixing may be important which introduces additional mass exchange coefficients. Numerically, this means that two additional transport equations for the concentrations in the two layers have to be solved. As an additional complication, it may be necessary from a physical point of view to introduce diffusion and viscous terms to account for horizontal exchange of mass and momentum. This changes the type of differential equations from hyperbolic to (incompletely) parabolic but it is believed that in such a case similar techniques to those described in this paper can still be used.

Acknowledgments

The major part of this work was done while the author stayed at the Department of Computer Science of the University of Uppsala (Sweden). Dr. Bertil Gustafsson and Dr. Björn Engquist of that institute contributed valuable ideas which are gratefully acknowledged.

References

1. F. Boulot, J. M. Parot, and J. P. Benque, IAHR Congress, Sao Paulo, 1975, C24, 199–209.
2. R. Courant and D. Hilbert, "Methods of Mathematical Physics, II," Interscience, New York, 1962.
3. S. Kanari, *Bull. Disaster Prevention Inst. Kyoto Univ.* **22** (1973), 69–96.
4. A. Kasahara, E. Isaacson, and J. J. Stoker, *Tellus* **17** (1965), 261–276.
5. H. O. Kreiss and J. Oliger, "Methods for the Approximate Solution of Time-Dependent Problems," GARP Publ. Series No. 10, World Meteor. Org., Geneva, 1973.
6. H. O. Kreiss and G. Scherer, Finite-element and finite-difference methods for hyperbolic partial differential equations, *in* "Mathematical Aspects of Finite Elements in Partial Differential Equations," pp. 195–212, Academic Press, New York, 1974.
7. J. M. Parot, *La Houille Blanche* **31** (1976), 53–58.
8. R. D. Richtmyer and K. W. Morton, "Difference Methods for Initial-Value Problems," 2nd ed., Interscience, New York, 1967.
9. G. Scherer, Thesis, Uppsala Univ., 1977.
10. A. Sundström, *Beitr. Phys. Atmosphare* **50** (1977), 218–224.
11. G. Veronis, *Deep-Sea Res.* **3** (1956), 157–177.
12. C. B. Vreugdenhil, Research Report No. S 114-VI, Delft Hydraulics Lab., March 1977.
13. J. D. Wang and J. J. Connor, Coastal Engineering Congr. 1974, Copenhagen, pp. 2401–2420.